

$\text{Nd}^{3+}$ ,  $3.62 \mu_{\text{B}}$ ;  $\text{Gd}^{3+}$ ,  $7.94 \mu_{\text{B}}$ )<sup>38</sup> and from those for their octahydrated sulfates,<sup>38</sup> suggesting that the 4f electrons in these complexed lanthanide ions are well-shielded by the outermost s and p electrons.

For the Gd complexes, whether monomeric or dimeric,  $\text{Gd}^{3+}$  has a  $4f^7$  configuration; since there is no orbital degeneracy associated with this configuration, the  $^8\text{S}$  ground term leads to a magnetic moment which is very close to the spin-only value ( $\mu_{\text{eff}} = g[S(S+1)]^{1/2} = 7.94 \mu_{\text{B}}$  per  $\text{Gd}^{3+}$ ), independent of ligand field effects. Magnetic susceptibility measurements were made on a powdered sample of  $[\text{Gd}(\text{L}1)]_2 \cdot 2\text{CHCl}_3$  over the temperature range 4.2–82 K. The effective magnetic moment at 81.7 K is, within error, identical to the spin-only value of  $7.94 \mu_{\text{B}}$  per  $\text{Gd}^{3+}$ . Below this temperature, the moment decreases slightly with decreasing temperature, becoming significantly less than the spin-only value by 30 K ( $7.81 \mu_{\text{B}}$ ) and reaching a value of  $7.30 \mu_{\text{B}}$  at 4.2 K. Since such behavior may arise from magnetic coupling between the metal centers in the dimer, the magnetic susceptibility data over the whole temperature range studied were compared to theory for two antiferromagnetically coupled  $S = 7/2$  ions.<sup>25</sup> Good agreement between experiment and theory was obtained for  $g = 2.00$  and  $-J = 0.045 (1) \text{ cm}^{-1}$ . There is evidence, then, for weak antiferromagnetic coupling in this compound although the strength of the coupling is clearly much less than that in any related homodinuclear lanthanide Schiff base compound.<sup>20</sup>

In conclusion, tripodal heptadentate amine phenol ligands have been prepared from  $\text{KBH}_4$  reduction of the corresponding Schiff bases. Reaction of these ligands with lanthanide nitrates yields type III dinuclear complexes in the presence of a base (hydroxide

or acetate), while type II complexes are obtained from the reactions of lanthanide nitrate with 1 equiv of the free ligand. Unlike mononuclear lanthanide complexes of heptadentate Schiff base ligands,<sup>4,5</sup> both types of complexes reported in this study are quite air-stable. From the structure of  $[\text{Gd}(\text{L}1)]_2 \cdot 2\text{CHCl}_3$ , it seems that the formation of the dinuclear complex is caused by the higher coordination requirements of lanthanide ions and/or by the small cavity of the heptadentate ligand. There are two ways to prevent this dimerization: one is to introduce bulky groups onto aromatic benzene rings at the 3-position and the other is to increase the length of three chelating "arms". Further studies on heptadentate tripod ligands with longer "arms" (to increase the cavity of the  $\text{N}_4\text{O}_3$  donor set) and with a variety of substituents on the aromatic rings (to modify the steric hindrance and lipophilicity) are in progress.

**Acknowledgment** is made to the Natural Sciences and Engineering Research Council of Canada for an NSERC Postdoctoral Fellowship (S.L.) and operating grants (R.C.T., C.O.) and to the U.S. Public Health Service for an operating grant (CA 48964). We also thank Professor J. Trotter for the use of his crystallographic facilities and Dr. P. Wassell for the use of his magnetometer for the room-temperature studies.

**Supplementary Material Available:** A more detailed table of crystallographic data (Table SI) and tables of hydrogen atom parameters (Table SII), anisotropic thermal parameters (Table SIII), torsion angles (Table SIV), intermolecular contacts (Table SV), least-squares planes (Table SVI), and final atomic coordinates and equivalent isotropic thermal parameters (Table SVIII) (17 pages); a listing of measured and calculated structure factor amplitudes (Table SVII) (45 pages). Ordering information is given on any current masthead page.

(38) Figgis, B. N. *Introduction to Ligand Fields*; Wiley Interscience: New York, 1961; p 326.

## Mechanism of Benzene Loss from $\text{Tp}'\text{Rh}(\text{H})(\text{Ph})(\text{CN-neopentyl})$ in the Presence of Neopentyl Isocyanide. Evidence for an Associatively Induced Reductive Elimination

William D. Jones\* and Edward T. Hessel

Contribution from the Department of Chemistry, University of Rochester, Rochester, New York 14627. Received January 6, 1992

**Abstract:** Thermolysis of  $\text{Tp}'\text{Rh}(\text{H})(\text{Ph})(\text{CN-neopentyl})$  (**1**) ( $\text{Tp}' = \text{hydrotris}(3,5\text{-dimethylpyrazolyl})\text{borate}$ ) in benzene in the presence of added isocyanide gives  $\text{Tp}'\text{Rh}(\text{CN-neopentyl})_2$  (**2**). The rate of reaction increases with increasing isocyanide concentration, but the dependence is nonlinear and approaches zero order at high isocyanide concentrations. When the reaction is conducted with  $\text{Tp}'\text{Rh}(\text{D})(d_5\text{-Ph})(\text{CN-neopentyl})$  in benzene- $d_6$ , an inverse kinetic isotope effect of  $0.85 \pm 0.02$  is observed. Measurement of the temperature dependence of the rate of the reaction at a single isocyanide concentration gives  $\Delta H^\ddagger = 15.2 \pm 1.2 \text{ kcal/mol}$  and  $\Delta S^\ddagger = -36 \pm 3 \text{ eu}$ . Thermolysis of **1** in the presence of added 2,6-xylyl isocyanide shows no evidence for the formation of  $\text{Tp}'\text{Rh}(\text{H})(\text{Ph})(2,6\text{-xylyl isocyanide})$  (**3**). Thermolysis of isotopically labeled  $\text{Tp}'\text{Rh}(\text{H})(d_5\text{-Ph})(\text{CN-neopentyl})$  at  $60^\circ\text{C}$  in either THF- $d_6$  or toluene- $d_8$  results in intramolecular migration of the metal hydride into all of the phenyl proton positions at the same time and rate. A mechanism is proposed to account for all of the above observations which involves initial reductive elimination of benzene from **1** to give an  $\eta^2$ -benzene intermediate in which the rhodium atom can migrate around the benzene ring. Subsequent associative exchange of isocyanide for benzene occurs in a second step.

### Introduction

The formation of a C–H bond by reductive elimination from a transition metal center is a fundamental process in organometallic chemistry<sup>1</sup> (eq 1) and is a crucial step in many reactions



catalyzed by homogeneous transition metal complexes.<sup>2</sup> Studies of the mechanism of this process for various systems have provided important insight into the requirements for the opposite reaction (i.e., oxidative addition of C–H bonds to a transition metal).<sup>3</sup>

(1) Halpern, J. *Acc. Chem. Res.* **1982**, *15*, 332. (b) Norton, J. R. *Acc. Chem. Res.* **1979**, *12*, 139.

(2) Chan, A. S. C.; Halpern, J. *J. Am. Chem. Soc.* **1980**, *102*, 838.

The mechanistic pathway for reductive elimination of an alkane or arene from mononuclear alkyl hydrido transition metal complexes can often depend on such factors as the type of metal, its ancillary ligands, and the concentration of complex in solution, as well as the concentration of added free ligands in solution. The reductive elimination of alkanes from octahedral complexes of rhodium or iridium typically requires prior dissociation of a neutral 2e donor ligand<sup>4</sup> whereas the reductive elimination of methane from Cp<sub>2</sub>Zr(H)(Me) involves initial coordination of a 2e donor ligand.<sup>5</sup> Loss of methane from the closely related Cp\*<sub>2</sub>Zr(H)(Me) proceeds by a more complex mechanism, in which initial  $\eta^5$  to  $\eta^4$  conversion of one Cp\* ligand of Cp\*<sub>2</sub>Zr(H)(CH<sub>3</sub>) is followed by intramolecular C-H oxidative addition of the other Cp\* ligand, all prior to reductive elimination of methane.<sup>6</sup>

The rate of reductive eliminations from square planar *cis*-alkylhydridoplatinum and -palladium complexes is unaffected by added 2e donor ligands.<sup>1a,7</sup> A similar effect is observed in the reductive elimination of methane from L<sub>2</sub>W(H)(Me) (L = Cp, Cp\*),<sup>8</sup> however, isotopic labeling studies suggest that an intermediate  $\sigma$ -alkane complex exists along the pathway to reductive elimination. At higher concentrations, an intermolecular hydride-exchange process makes the reductive elimination appear to be intermolecular. The intramolecularity of the reductive elimination of methane from Os(H)(Me)(CO)<sub>4</sub> is dependent on the concentration of added triphenylphosphine.<sup>1b,9</sup> Intramolecular reductive elimination has also been reported for Ru(PPh<sub>3</sub>)<sub>3</sub>(CO)(H)(R), in which subsequent ortho metalation of a triphenylphosphine ligand is observed.<sup>10</sup>

Most relevant to the results to be presented in this paper is the mechanism of reductive elimination of alkanes and arenes from complexes of the type Cp\*M(PMe<sub>3</sub>)(R)(H) (M = rhodium, iridium).<sup>11</sup> Reductive elimination of R-H results in the formation of a coordinatively unsaturated 16e intermediate which can either be trapped by a neutral 2e donor ligand or undergo reaction with the C-H bonds of the solvent. As with complexes of the type Cp<sub>2</sub>W(H)(R), there is strong evidence for the existence of  $\sigma$ -alkane complexes along the pathway to reductive elimination.<sup>11b,12</sup> For reductive elimination of benzene from Cp\*Rh(H)(Ph)(PMe<sub>3</sub>), it has been established that there is an  $\eta^2$ -benzene intermediate.<sup>11d</sup> Although the majority of the above mentioned examples involve

Table I. Rates and Free Energies of Activation for Benzene Exchange in **1** at Various Temperatures

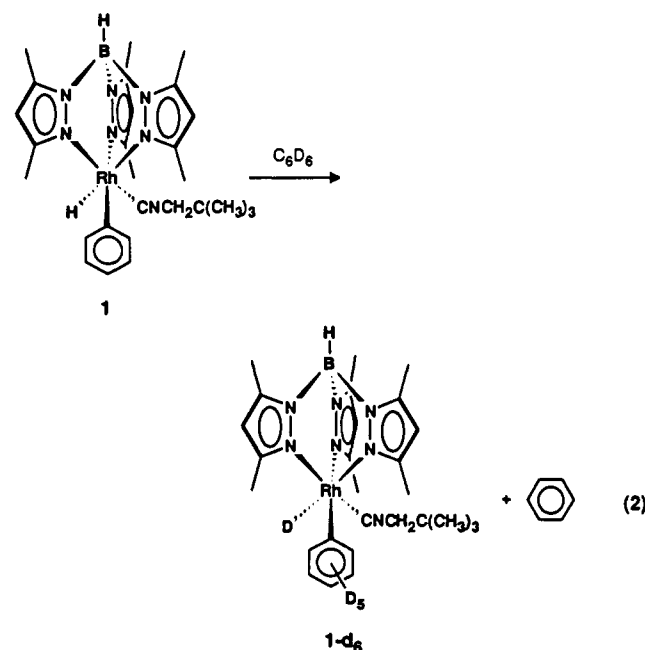
temp (K)	$k_{\text{obs}}$ (s <sup>-1</sup> )	$\Delta G^\ddagger$ (kcal/mol)	temp (K)	$k_{\text{obs}}$ (s <sup>-1</sup> )	$\Delta G^\ddagger$ (kcal/mol)
353	2.7 (1) $\times 10^{-6}$	29.77 (2)	373	5.4 (2) $\times 10^{-5}$	29.28 (3)
367	2.6 (2) $\times 10^{-5}$	29.33 (6)	386	3.0 (4) $\times 10^{-4}$	29.01 (10)

reductive elimination from mononuclear metal centers, it should be noted that reductive elimination of alkanes from binuclear complexes is known<sup>13</sup> as well as bimolecular reductive eliminations from L<sub>n</sub>M(R) and L<sub>n</sub>M(H).<sup>14</sup>

In this paper we report the results of an investigation into the thermolysis of Tp'Rh(H)(Ph)(CN-neopentyl) (**1**) (Tp' = hydrotris(3,5-dimethylpyrazolyl)borate) in the presence of neopentyl isocyanide to give Tp'Rh(CN-neopentyl)<sub>2</sub> (**2**) and benzene. Although there is much evidence that the Cp\* and Tp' ligands are both electronically and sterically similar, the reductive elimination of benzene from **1** is distinctly different from that observed for the closely related Cp\*Rh(H)(Ph)(PMe<sub>3</sub>). The results of kinetics experiments indicate that both isocyanide coordination and reductive elimination of benzene occur before or during the rate-determining step and that at least one intermediate exists along the reaction pathway. An isotopic labeling study has helped to establish the identity of the intermediate.

## Results and Discussion

**Benzene-Exchange Reaction of Tp'Rh(H)(Ph)(CN-neopentyl).** Heating a solution of Tp'Rh(H)(Ph)(CN-neopentyl) (**1**) in benzene-*d*<sub>6</sub> results in the production of 1-*d*<sub>6</sub> along with free benzene (eq 2). The rate of the reaction was measured at various tem-



peratures by monitoring the decrease in the hydride resonance in the <sup>1</sup>H NMR spectrum of **1** over time. Plots of ln [**1**] vs time allowed for the determination of the first-order rate of benzene exchange and  $\Delta G^\ddagger$  at each temperature (Table I).  $\Delta G^\ddagger$  is relatively constant over the temperature range of the study, with the values being slightly higher than those measured for the reductive elimination of benzene from the related complexes Cp\*Rh(H)(Ph)(PMe<sub>3</sub>) (25–26 kcal/mol)<sup>11d</sup> and Tp'Rh(H)(Ph)(CO) (~25 kcal/mol).<sup>15</sup> However, it should be noted that these studies

(3) Halpern, J. *Inorg. Chim. Acta* **1985**, *100*, 41.

(4) (a) Milstein, D. *J. Am. Chem. Soc.* **1982**, *104*, 5227. (b) Milstein, D. *Acc. Chem. Res.* **1984**, *17*, 221. (c) Longato, B.; Bresadola, S. *Inorg. Chem.* **1982**, *21*, 168. (d) Basato, M.; Morandini, F.; Longato, B.; Bresadola, S. *Inorg. Chem.* **1984**, *23*, 649. (e) Basato, M.; Morandini, F.; Longato, B.; Bresadola, S. *Inorg. Chem.* **1984**, *23*, 3972. Prior ligand dissociation is not a required mechanism for octahedral complexes of rhodium and iridium: Thompson, J. S.; Bernard, K. A.; Rappoli, B. J.; Atwood, J. D. *Organometallics* **1990**, *9*, 2727.

(5) Yoshifuji, M.; Gell, K. I.; Schwartz, J. J. *Organomet. Chem.* **1978**, *153*, C15. Gell, K. I.; Schwartz, J. J. *J. Chem. Soc., Chem. Commun.* **1979**, 244. Gell, K. I.; Schwartz, J. J. *Organomet. Chem.* **1978**, *162*, C11. Gell, K. I.; Schwartz, J. J. *J. Am. Chem. Soc.* **1978**, *100*, 3246.

(6) McAlister, D. R.; Erwin, D. K.; Bercaw, J. E. *J. Am. Chem. Soc.* **1978**, *100*, 5966.

(7) (a) Abis, L.; Sen, A.; Halpern, J. J. *J. Am. Chem. Soc.* **1978**, *100*, 2915. (b) Michelin, R. A.; Faglia, S.; Uguagliati, P. *Inorg. Chem.* **1983**, *22*, 1831. (c) Hackett, M.; Whitesides, G. M. *J. Am. Chem. Soc.* **1988**, *110*, 1449. (d) Sostero, S.; Traverso, O.; Ros, R.; Michelin, R. A. *J. Organomet. Chem.* **1983**, *246*, 325.

(8) (a) Bullock, M. R.; Headford, C. E. L.; Kegley, S. E.; Norton, J. R. *J. Am. Chem. Soc.* **1985**, *107*, 727. (b) Headford, C. E. L.; Hennessy, K. M.; Kegley, S. E.; Norton, J. R. *J. Am. Chem. Soc.* **1989**, *111*, 3897. (c) Cooper, N. J.; Green, M. L. H.; Mahtab, R. J. *J. Chem. Soc., Dalton Trans.* **1979**, 1557.

(9) (a) Carter, W. J.; Okrasinski, S. J.; Norton, J. R. *Organometallics* **1985**, *4*, 1376. (b) Okrasinski, S. J.; Norton, J. R. *J. Am. Chem. Soc.* **1977**, *99*, 295. (c) Norton, J. R. *Acc. Chem. Res.* **1979**, *12*, 139.

(10) Roper, W. R.; Wright, L. J. *J. Organomet. Chem.* **1982**, *234*, C5.

(11) (a) Wax, M. J.; Stryker, J. M.; Buchanan, J. M.; Kovac, C. A.; Bergman, R. G. *J. Am. Chem. Soc.* **1984**, *106*, 1121. (b) Buchanan, J. M.; Stryker, J. M.; Bergman, R. G. *J. Am. Chem. Soc.* **1986**, *108*, 1537. (c) Janowicz, A. H.; Bergman, R. G. *J. Am. Chem. Soc.* **1983**, *105*, 3929. (d) Jones, W. D.; Feher, F. J. *J. Am. Chem. Soc.* **1984**, *106*, 1650. Jones, W. D.; Feher, F. J. *Acc. Chem. Res.* **1989**, *22*, 91. Belt, S. T.; Dong, L.; Duckett, S. B.; Jones, W. D.; Partridge, M. G.; Perutz, R. N. *J. Chem. Soc., Chem. Commun.* **1991**, 264.

(12) Periana, R. A.; Bergman, R. G. *J. Am. Chem. Soc.* **1986**, *108*, 7332.

(13) (a) Kellenberger, B.; Young, S. J.; Stille, J. K. *J. Am. Chem. Soc.* **1985**, *107*, 6105. (b) Azam, K. A.; Puddephatt, R. J. *Organometallics* **1983**, *2*, 1369.

(14) (a) Halpern, J. *Inorg. Chim. Acta* **1982**, *62*, 31. (b) Nappa, M. J.; Santi, R.; Diefenbach, S. P.; Halpern, J. J. *J. Am. Chem. Soc.* **1982**, *104*, 619. (c) Nappa, M. J.; Santi, R.; Halpern, J. *Organometallics* **1985**, *4*, 34. (d) Jones, W. D.; Bergman, R. G. *J. Am. Chem. Soc.* **1979**, *101*, 5447.

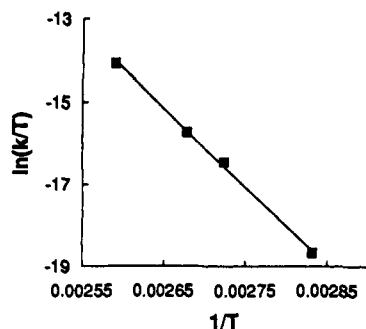
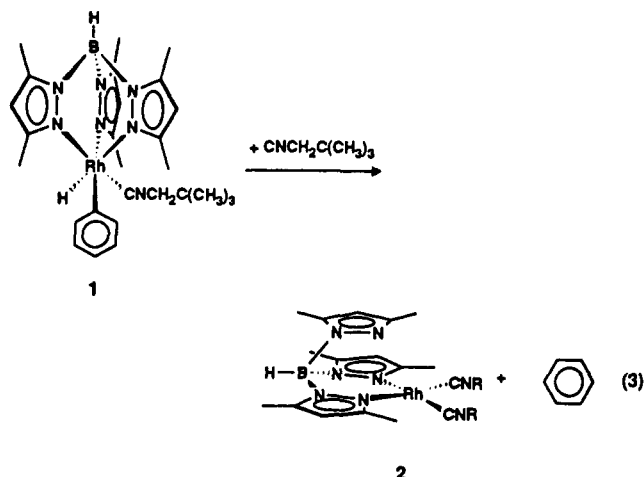


Figure 1. Plot of  $\ln(k/T)$  vs  $1/T$  for benzene exchange in Tp'Rh(H)(Ph)(CN-neopentyl) (1).

were conducted at lower temperatures (20–40 °C) than the present study. An Eyring plot of the rate data (Figure 1) gives  $\Delta H^\ddagger = 37.8 \pm 1.1$  kcal/mol and  $\Delta S^\ddagger = 23 \pm 3$  eu. The enthalpy of activation is significantly higher than previously reported values for reductive elimination of benzene from similar complexes ( $\sim 30$  kcal/mol).<sup>11d,15</sup>

**Kinetics Studies of the Thermolysis of Tp'Rh(H)(Ph)(CN-neopentyl) in the Presence of Neopentyl Isocyanide.** When **1** is heated in the presence of excess neopentyl isocyanide (0.167 M), product **2** is formed along with 1 equiv of benzene (eq 3).



Comparison of the rate of disappearance of **1** in reaction 3 ( $3.0 (3) \times 10^{-4} \text{ s}^{-1}$ ) with the rate of disappearance of **1** during the thermolysis of **1** alone in benzene-*d*<sub>6</sub> at 94 °C ( $2.6 (2) \times 10^{-5} \text{ s}^{-1}$ , eq 2) shows that the rate of reaction 3 is significantly faster (Figure 2). Thus it is immediately evident that the rate of loss of benzene from **1** is affected by added isocyanide. To obtain a more complete picture of this effect, the rate of reaction 3 was monitored by UV-vis spectroscopy at 372 nm at various concentrations of isocyanide at 82 °C (Table II).<sup>16</sup> A plot of rate vs isocyanide concentration is nonlinear and appears to approach a saturation rate at high concentrations of isocyanide (Figure 3a). Efforts to observe the saturation point by conducting reactions at higher concentrations of isocyanide (>0.5 M) were not reproducible due to large fluctuations in the baseline absorption in the area of 372 nm. This effect is presumably due to the isocyanide, since absorption measurements of a 1.0 M solution of neopentyl isocyanide alone in benzene at 82 °C showed similar radical behavior. However, a double-reciprocal plot of  $1/k_{\text{obs}}$  vs  $1/[\text{CN-neopentyl}]$  for the available data in Table II is linear (Figure 3b).

The thermodynamic parameters for reaction 3 were determined by following the rate of the reaction ( $[\text{CN-neopentyl}] = 104 \text{ mM}$ ) at various temperatures (Table III). From the Eyring plot of

(15) Ghosh, C. K. Ph.D. Dissertation, University of Alberta, 1988.

(16) Complex **2** is bright yellow and possesses strong absorptions at both 302 and 372 nm. The rate of formation of **2** can be determined by monitoring the rate of change of the absorbance at 372 nm over time. Attempts to monitor reactions at 302 nm were less successful, since neopentyl isocyanide possesses a significant absorbance in that region.

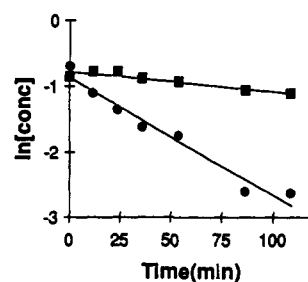


Figure 2. Plots of  $\ln[1]$  vs time for Tp'Rh(H)(Ph)(CN-neopentyl) alone in benzene (■) and Tp'Rh(H)(Ph)(CN-neopentyl) in benzene with 0.167 M neopentyl isocyanide (●).

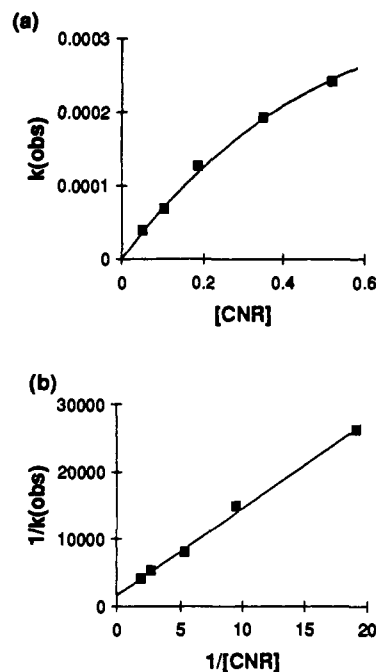


Figure 3. Plots of (a)  $k_{\text{obs}}$  vs concentration of neopentyl isocyanide and (b)  $1/k_{\text{obs}}$  vs  $1/[\text{neopentyl isocyanide}]$  for conversion of Tp'Rh(H)(Ph)(CN-neopentyl) (1) to Tp'Rh(CN-neopentyl)<sub>2</sub> (2) in benzene.

Table II. Rate of Formation of **2** as a Function of Neopentyl Isocyanide Concentration at 82 °C in Benzene

isocyanide concn (mM)	$k_{\text{obs}}$ ( $\text{s}^{-1}$ )	isocyanide concn (mM)	$k_{\text{obs}}$ ( $\text{s}^{-1}$ )
52	$3.82 (1) \times 10^{-5}$	353	$1.93 (2) \times 10^{-4}$
104	$6.74 (2) \times 10^{-5}$	520	$2.41 (4) \times 10^{-4}$
186	$1.26 (1) \times 10^{-4}$		

Table III. Rates and Free Energies of Activation for Formation of **2** from **1** in 104 mM Neopentyl Isocyanide in Benzene at Various Temperatures

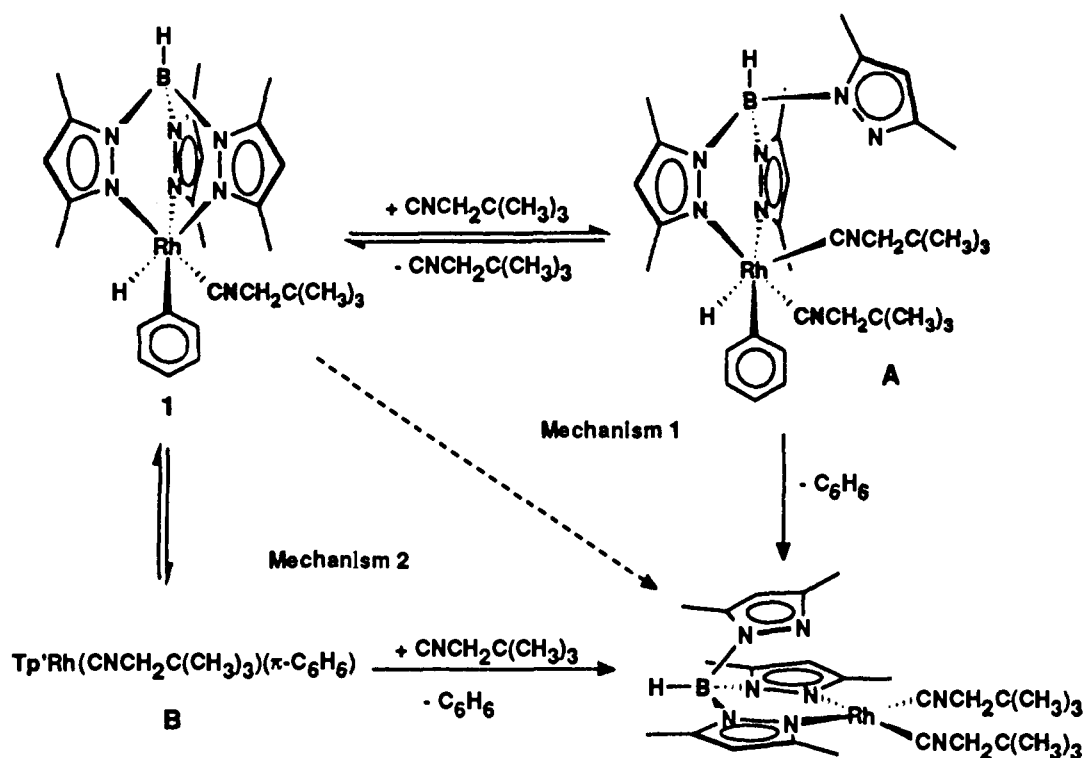
temp (K)	$k_{\text{obs}}$ ( $10^{-5} \text{ s}^{-1}$ )	$\Delta G^\ddagger$ (kcal/mol)	temp (K)	$k_{\text{obs}}$ ( $10^{-5} \text{ s}^{-1}$ )	$\Delta G^\ddagger$ (kcal/mol)
338	1.68 (7)	27.2 (3)	350	4.10	27.62 (1)
343	2.68 (6)	27.35 (1)	356	5.66 (1)	27.88 (1)

Table IV. Rates of Formation of **2** from **1-d**<sub>6</sub> and **1** in Benzene in the Presence of 104 mM Neopentyl Isocyanide at 82 °C

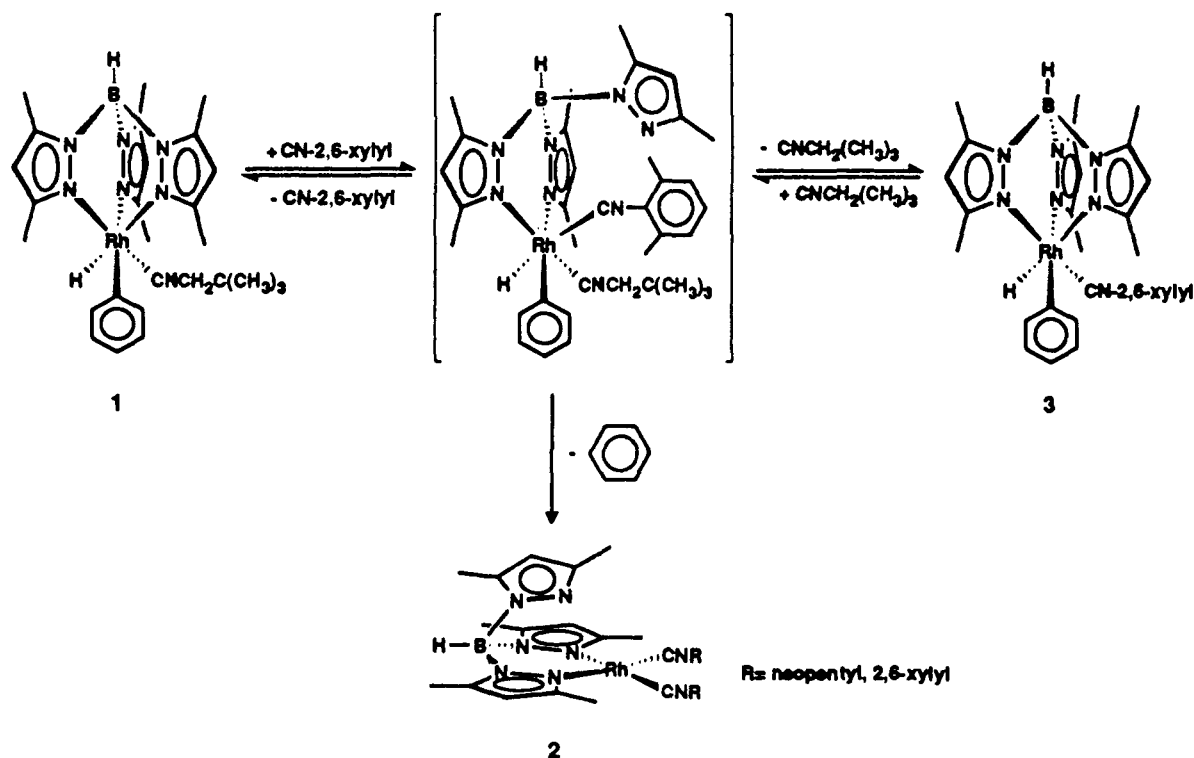
reaction	$k_{\text{obs}}$ ( $10^{-5} \text{ s}^{-1}$ )	reaction	$k_{\text{obs}}$ ( $10^{-5} \text{ s}^{-1}$ )
<b>1-d</b> <sub>6</sub> in benzene- <i>d</i> <sub>6</sub>	7.57 (5)	<b>1</b> in benzene	6.66 (4)
	7.7 (1)		6.74 (2)
	8.03 (7)		

the data,  $\Delta H^\ddagger$  and  $\Delta S^\ddagger$  for reaction 3 were determined to be  $15.2 \pm 1.2$  kcal/mol and  $-36 \pm 3$  eu, respectively (Figure 4). The large negative  $\Delta S^\ddagger$  contrasts with that observed for the simple exchange of benzene discussed above (eq 2) and points toward

Scheme I



Scheme II



an associative reaction prior to or during the rate-determining step for the reaction with isocyanide.

When the reaction of eq 3 is conducted using  $\text{Tp}'\text{Rh}(\text{D})(d_5\text{-Ph})(\text{CN-neopentyl})$  ( $1-d_6$ ) in benzene- $d_6$ , the rate of the reaction increases. The observed kinetic isotope effect of  $k_1/k_d = 0.85 \pm 0.02$  was determined from an average of rates for the reactions listed in Table IV. A small and inverse isotope effect is consistent with previously determined values measured for arene reductive eliminations<sup>17</sup> and shows that C-H bond formation occurs before

or during the rate-determining step for reaction 3.

**Mechanistic Investigations.** With the information from the above experiments, it is possible to propose two general associative mechanisms for reaction 3 as shown in Scheme I. Both mechanisms would be predicted to show a dependence on the isocyanide concentration and are expected to possess a primary inverse isotope effect. Additionally, both mechanisms involve an intermediate in equilibrium with 1, as is suggested from the observed nonlinear dependence of isocyanide concentration on the rate of reaction 3. The difference in the mechanisms is that in mechanism 1 isocyanide reacts with 1 to generate an intermediate whereas in mechanism 2 isocyanide reacts with an intermediate formed by

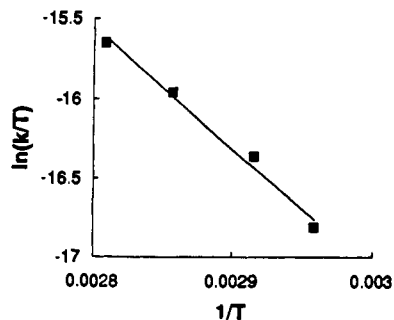


Figure 4. Plot of  $\ln(k/T)$  vs  $1/T$  for conversion of  $Tp^*Rh(H)(Ph)(CN\text{-neopentyl})$  (1) to  $Tp^*Rh(CN\text{-neopentyl})_2$  (2) in benzene.

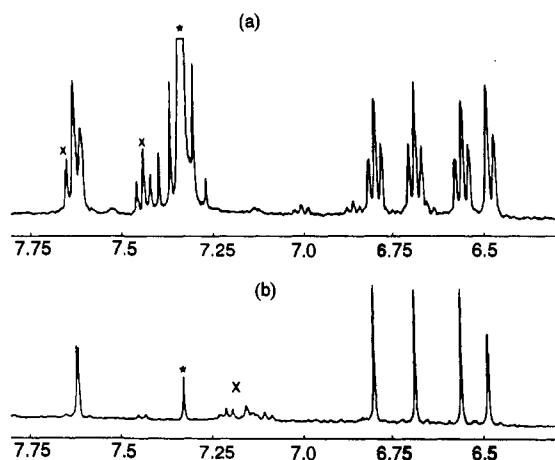


Figure 5.  $^1H$  NMR spectra of (a)  $Tp^*Rh(H)(Ph)(CN\text{-neopentyl})$  (1) and (b) equilibrium mixture of five possible isotopomers of  $Tp^*Rh(H)(d_5\text{-Ph})(CN\text{-neopentyl})$  ( $1\text{-}d_5$ ) in the phenyl region ( $\delta$  6.3–7.8) in  $THF\text{-}d_8$  at  $-35^\circ C$  (impurities are marked with an  $\times$ ; residual benzene is marked with an  $*$ ).

rearrangement of **1**. Also, saturation of the rate in mechanism 1 would be associated with the buildup of intermediate A, which should be observable at high isocyanide concentrations.

Mechanism 1 involves substitution of one pyrazole ring of the  $Tp^*$  ligand by an isocyanide, most likely by a dissociative pathway. Rate-determining reductive elimination of benzene from intermediate A is irreversible. A key point of this mechanism is that the coordinated isocyanide can undergo slow exchange with free isocyanide in solution via intermediate A of Scheme I. To test for isocyanide exchange in **1**, the complex  $Tp^*Rh(H)(Ph)(CN\text{-}2,6\text{-xylyl})$  (**3**) was prepared independently by photolysis of  $Tp^*Rh(CN\text{-}2,6\text{-xylyl})(\eta^2\text{-PhN}=\text{C}=\text{N}\text{-}2,6\text{-xylyl})$  (**4**) in benzene. Complex **3** possesses a hydride resonance in the  $^1H$  NMR spectrum at  $\delta$   $-13.251$  at  $60^\circ C$  in benzene- $d_6$ . The hydride resonance for **1** is located at  $\delta$   $-13.801$ , and thus it should be possible to detect **3** in a benzene- $d_6$  solution of **1** at  $60^\circ C$  if it is formed by isocyanide exchange (Scheme II). Accordingly, a benzene- $d_6$  solution of **1** containing 10 equiv of added 2,6-xylyl isocyanide in a sealed NMR tube was heated at  $60^\circ C$  in the NMR probe. At no time during the conversion of **1** to a mixture of  $Tp^*Rh(CNR)_2$  ( $R = \text{equilibrium mixture of neopentyl and } 2,6\text{-xylyl}$ ) was there observed a resonance at  $\delta$   $-13.251$ , indicating that isocyanide exchange into **1** does not occur. In addition, no direct evidence for the buildup of intermediate A was seen in the reactions with neopentyl isocyanide.

In mechanism 2, reductive elimination to give a  $\pi$ -benzene complex (vide infra) precedes complexation of isocyanide. Reversible reductive elimination of benzene is followed by rate-determining bimolecular displacement of the  $\pi$ -coordinated benzene by isocyanide from intermediate B. If an intermediate such as B were formed reversibly along the pathway of reaction 3, it should be possible to observe evidence of exchange of the hydride proton with the phenyl protons in **1**. Previous studies have demonstrated the existence of an  $\eta^2$ -benzene intermediate in the reductive

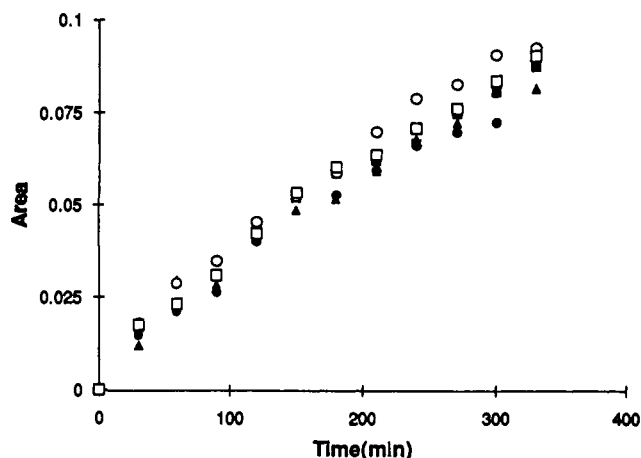


Figure 6. Plots of the increase in the areas of the phenyl resonances of  $Tp^*Rh(H)(d_5\text{-Ph})(CN\text{-neopentyl})$  vs time at  $60^\circ C$  in  $THF\text{-}d_8$ :  $\blacksquare$ , ortho;  $\bullet$ , meta;  $\blacktriangle$ , para;  $\circ$ , meta';  $\square$ , ortho'.

Table V. Rates of Hydride Migration into the Phenyl Positions of  $1\text{-}d_5$

position, $\delta$ (ppm)	$k_{\text{obs}}$ ( $10^{-5} \text{ s}^{-1}$ )	position, $\delta$ (ppm)	$k_{\text{obs}}$ ( $10^{-5} \text{ s}^{-1}$ )
ortho, 6.484	3.4 (1)	meta', 6.801	3.9 (9)
meta, 6.558	3.3 (2)	ortho', 7.619	3.6 (1)
para, 6.684	3.2 (1)	hydride, $-13.650$	3.9 (1)

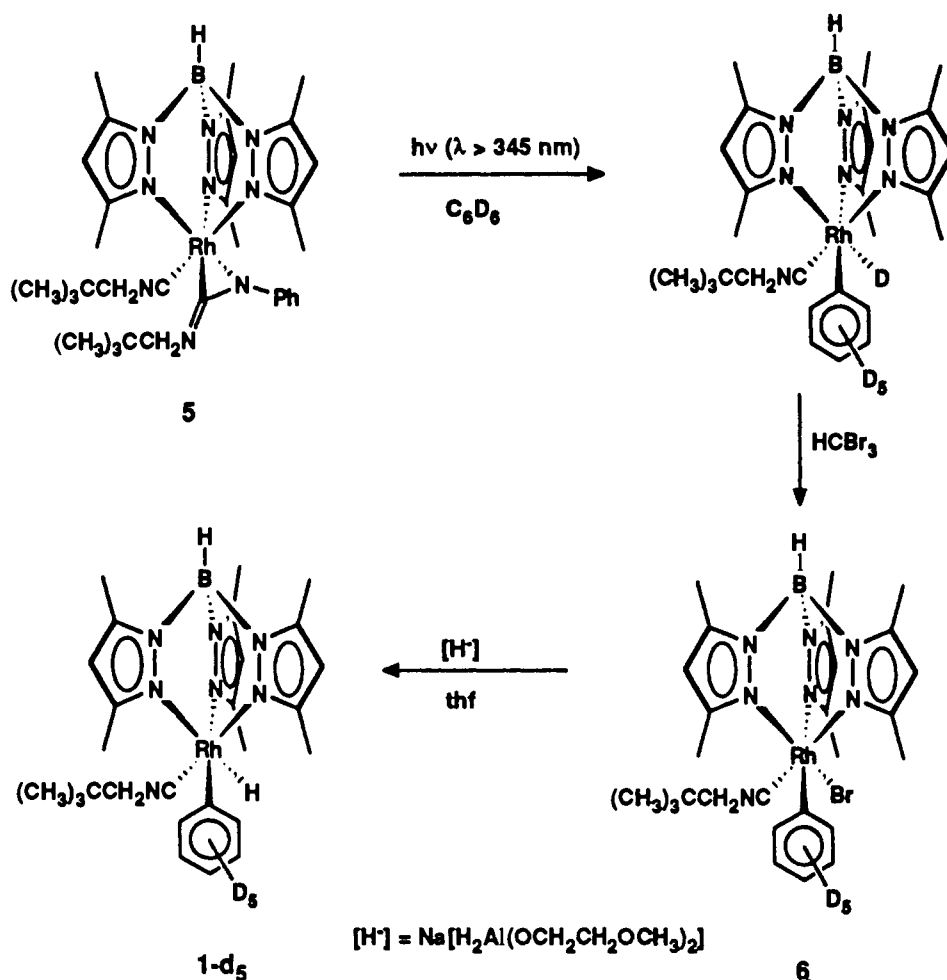
elimination of benzene from  $Cp^*Rh(H)(Ph)(PMe_3)$  by both direct isotopic labeling and spin-saturation-transfer experiments.<sup>11d</sup> Attempts to use spin-saturation transfer as a tool for observing the equilibration of the hydride proton with the phenyl protons of **1** were not successful because hindered rotation of the phenyl ring in **1** at  $100^\circ C$  (the temperature at which the rate of exchange was predicted to be sufficiently fast to be observed) broadened the phenyl resonances. However, a temperature-dependent  $^1H$  NMR study of the hindered rotation of the phenyl ring of **1** in  $THF\text{-}d_8$  indicates that the process reaches the slow-exchange limit at  $-36^\circ C$ , and so direct observation of hydride migration into the phenyl ring of **1** would be possible if a specifically labeled complex could be successfully prepared.

Accordingly, the complex  $Tp^*Rh(H)(d_5\text{-Ph})(CN\text{-neopentyl})$  ( $1\text{-}d_5$ ), containing a deuterated phenyl ring, was prepared as illustrated in Scheme III. Photolysis of  $Tp^*Rh(CN\text{-neopentyl})(\eta^2\text{-PhN}=\text{C}=\text{N}\text{-neopentyl})$  (**5**) in benzene- $d_6$  produces  $Tp^*Rh(D)(C_6D_5)(CN\text{-neopentyl})$  ( $1\text{-}d_6$ ) in quantitative yield as determined by a  $^1H$  NMR spectrum of the products. Addition of an excess of bromoform to the reaction gives  $Tp^*Rh\text{-}(Br)(C_6D_5)(CN\text{-neopentyl})$  (**6**), which is isolated in 70% yield after purification by preparative thin-layer chromatography.<sup>18</sup> Reaction of **6** with several equivalents of  $NaH_2Al(OCH_2CH_2OCH_3)_2$  (Red-Al) in THF at  $25^\circ C$  gives the desired isotopically labeled complex  $1\text{-}d_5$  in 60% overall yield from **5**.

When complex  $1\text{-}d_5$  is heated in  $THF\text{-}d_8$  at  $60^\circ C$ , slow migration of the hydride into the phenyl positions is observed by  $^1H$  NMR spectroscopy. The spectrum of the mixture of the isotopically labeled isomers of  $1\text{-}d_5$  at equilibrium (after heating at  $60^\circ C$  for  $\sim 1100$  h) at  $-45^\circ C$  consists of five singlets located at the identical chemical shifts as the phenyl resonances of **1** (Figure 5). The rate of migration of the hydride proton into the phenyl ring was measured by heating a sample of  $1\text{-}d_5$  in  $THF\text{-}d_8$  in a sealed NMR tube at  $60^\circ C$  in an oven and removing the sample periodically to obtain a  $^1H$  NMR spectrum in a cooled probe at  $-45^\circ C$ . A plot of the increase of each of the phenyl resonances over time is shown in Figure 6. It is important to note that the hydride label is observed in all of the possible positions of the phenyl ring at the same time. This will become important

(18) Reaction of bromoform with the B-H bond of the  $Tp^*$  ligand presumably accounts for the low yield of **6**.

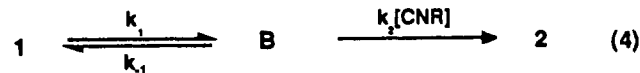
Scheme III



later in the discussion of the nature of intermediate B. Logarithmic plots of the hydride and phenyl resonances of  $1-d_5$  are linear, giving similar rate constants as indicated in Table V.

As a check for intramolecularity of the migration, 50 equiv of benzene- $d_6$  was added to an equilibrium mixture of the isotopically labeled isomers of  $1-d_5$  in THF- $d_8$ . The solution was heated at 60 °C, and  $^1\text{H}$  NMR spectra were obtained as before at -45 °C. The spectra showed no significant change in the integration of the resonances associated with the hydride or phenyl group and no formation of free benzene- $d_5$  after 15 h of heating. Additionally, when  $1-d_5$  was heated at 60 °C in toluene- $d_8$ , the first-order rate of migration of the hydride was  $4.9 (2) \times 10^{-5} \text{ s}^{-1}$  (slightly faster than in THF), with no formation of free benzene- $d_5$  observed. Hence, the proton migration within  $1-d_5$  is intramolecular.

The observation of migration of the hydride resonance into the phenyl ring of **1** confirms that reductive elimination/oxidative addition of benzene is a rapid and reversible process; however, it does not necessarily prove that an intermediate of type B is along the pathway to formation of **2**. Consideration of the kinetic rate law for mechanism 2 of Scheme I (eq 4) indicates that the dou-



$$k_{\text{obs}} = \frac{k_1 k_2 [\text{CNR}]}{k_{-1} + k_2 [\text{CNR}]} \quad \text{or} \quad \frac{1}{k_{\text{obs}}} = \frac{1}{k_1} + \frac{k_{-1}}{k_1 k_2 [\text{CNR}]}$$

ble-reciprocal plot of the rate of reaction 2 as a function of the concentration of isocyanide (Figure 3b) should give as a  $y$ -intercept the reciprocal of the forward rate constant ( $k_1$ ) for the formation of intermediate B. Neglecting isotope effects,<sup>19</sup> the observed rate

for the disappearance of the hydride in the migration experiment of  $1-d_5$  should also correspond to  $k_1$  (see Experimental Section). Unfortunately, the hydride migration experiment was conducted at 60 °C, while all of the isocyanide dependence reactions were conducted at 82 °C. By assuming that  $\Delta G^\ddagger$  is constant over the temperature range 60–82 °C, it is possible to estimate the rate of the hydride migration at 82 °C and compare it to the rate abstracted from the double-reciprocal plot of the isocyanide dependence study as outlined below.

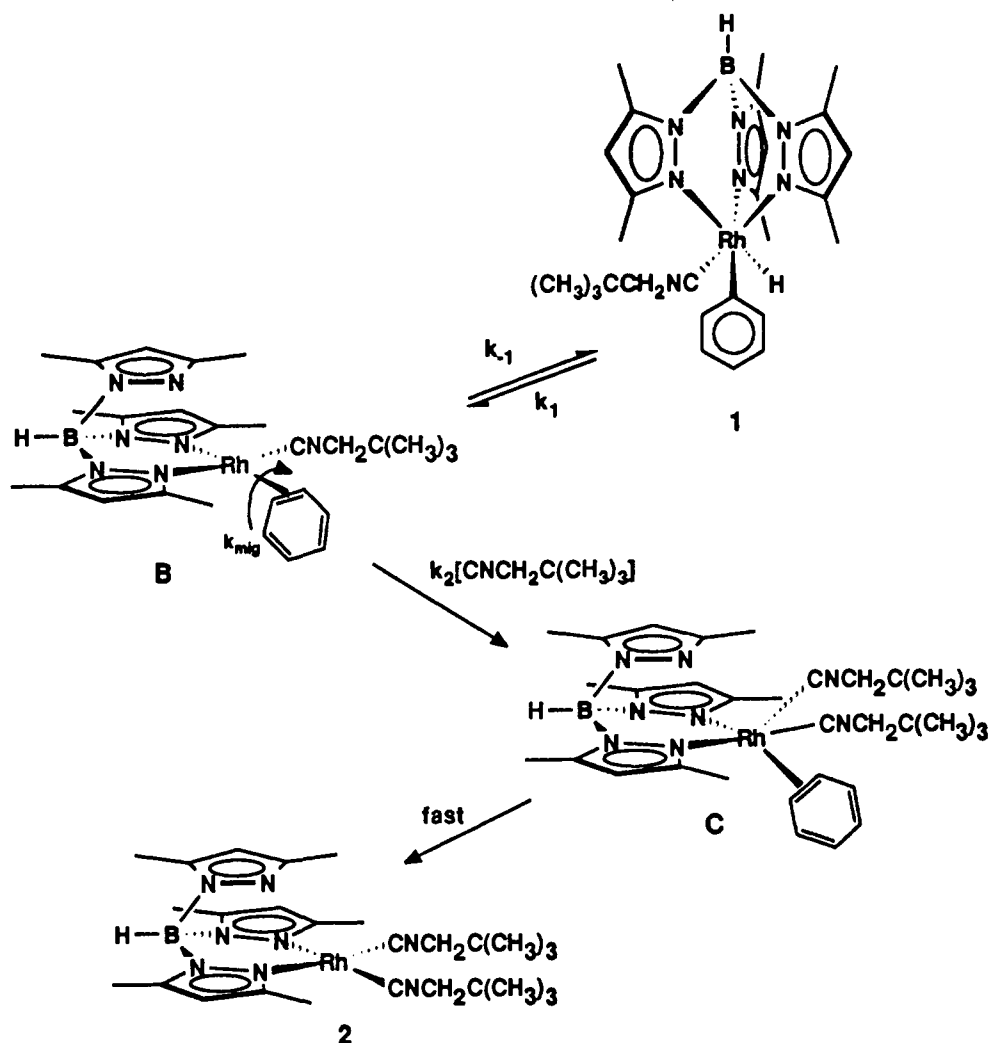
The rate of migration of the hydride of  $1-d_5$  at 60 °C in toluene is  $9.1 (1) \times 10^{-5} \text{ s}^{-1}$ . The corresponding rate at 82 °C is estimated from the Eyring equation (using  $\Delta G^\ddagger$  for 60 °C) to be  $1.1 (1) \times 10^{-3} \text{ s}^{-1}$ . Despite the crudeness of the estimate, this rate is within a factor of 2 of the predicted rate of  $6 (2) \times 10^{-4} \text{ s}^{-1}$ , extracted from the inverse of the  $y$ -intercept of the double-reciprocal plot of Figure 3b. Thus the correlation in rates between the two independent experiments indicates that the  $\pi$ -benzene intermediate B is along the pathway to **2**.

As mentioned earlier, the activation parameters for the reaction of **1** with neopentyl isocyanide were measured at  $[\text{CNR}] = 0.104 \text{ M}$ . At this concentration, the  $k_1/k_{-1}$  equilibrium is rapid and reversible compared to the reaction with isocyanide (the rate falls in the linear portion of Figure 3a). Consequently, these parameters reflect changes not only due to the formation of the  $\eta^2$ -benzene ligand but also due to the coordination of free isocyanide. The large negative  $\Delta S^\ddagger$  is consistent with this combination of reaction steps.

Similarly, the isotope effect studies provide observed rate constants that reflect both of these steps. The  $k_{\text{H}}/k_{\text{D}}$  ratio will depend on the net differences in Rh-H, Rh-D, C-H, and C-D bonding in the ground state and the rate-determining transition

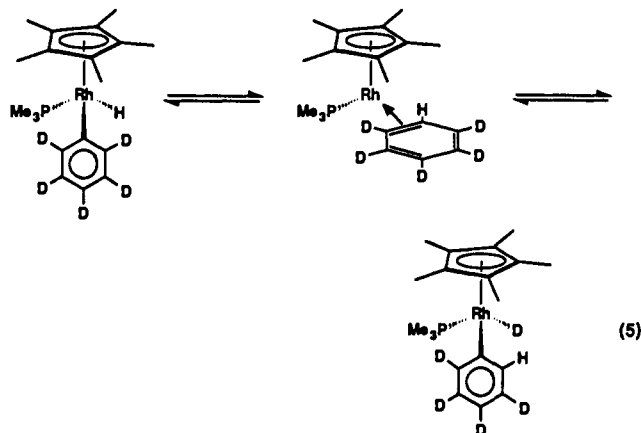
(19) These effects would tend to favor keeping deuterium attached to carbon and would be expected to be small (0.6–1.3).<sup>17</sup>

Scheme IV



states. The second step, involving isocyanide coordination, would be expected to have little isotope effect associated with it, and consequently the observed  $k_H/k_D$  ratio most likely reflects the effect of deuterium substitution on the  $k_1/k_{-1}$  equilibrium.

A major issue still to be considered is the identity of intermediate **B**. In the hydride migration experiment with  $1-d_5$ , it was observed that the hydride migrated into each of the possible phenyl proton positions at the same time and rate. Certainly this type of migration is inconsistent with an  $\eta^2$ -benzene intermediate and 1,2-shifts, as was observed by Jones and Feher with  $Cp^*Rh(H)(Ph)(PMe_3)^{17}$  (eq 5). Such an intermediate should only incor-



porate label into the ortho positions of the phenyl ring during the initial stages of the migration. However, an equilibrium between

$\eta^2$ -benzene and  $\eta^4$ -benzene intermediates would allow for equal incorporation of proton label into all possible positions of the phenyl ring in  $1-d_5$ . A more reasonable and less formal alternative of this equilibrium is shown in the proposed mechanism for reaction 3 in Scheme IV and involves a fluxional  $\eta^2$ -benzene intermediate in which the rhodium atom rapidly migrates around the  $\pi$ -system of the benzene ring. It should be emphasized that  $k_{mig}$  must be rapid with respect to  $k_{-1}$  in Scheme IV for random scrambling of label throughout all possible sites to occur.

A detail of the mechanism of reaction 3 which has been more or less ignored until this point concerns the known change in hapticity of the  $Tp^*$  ligand that occurs in going from **1** to **2**. Although no formal probe of this aspect of the reaction was conducted, it is generally observed that  $Tp^*Rh(CNR)$  complexes that contain a formally rhodium(III) metal atom have an  $\eta^3$ - $Tp^*$  ligand whereas formally rhodium(I) square planar complexes possess an  $\eta^2$ - $Tp^*$  ligand.<sup>20,21</sup> Thus it seems reasonable that any  $\pi$ -benzene intermediates along the pathway to **2** should have an  $\eta^2$ - $Tp^*$  ligand as shown in Scheme IV. But the question still remains as to whether the change in hapticity is concerted with reductive elimination of benzene or actually occurs as a step prior to reductive elimination, as is well-known for octahedral complexes of rhodium.<sup>4</sup> Further investigations in regard to hapticity changes of the  $Tp^*$  ligand would be helpful in providing a clearer picture of reductive elimination of R-H in these complexes.

It is also interesting to consider the microscopic reverse of Scheme IV. The thermal activation of benzene by  $Tp^*Rh(CN\text{-neopentyl})_2$  should proceed by way of initial  $\pi$ -coordination of

(20) Jones, W. D.; Hessel, E. T. *Inorg. Chem.* **1991**, *30*, 778.

(21) Jones, W. D.; Hessel, E. T. *Organometallics* **1992**, *11*, 1496.

benzene, giving intermediate C followed by loss of isocyanide to give B. Oxidative addition to the C-H bond occurs next, followed by  $\eta^2$ - to  $\eta^3$ -coordination of the Tp' ligand. The largest barrier in this sequence is the loss of isocyanide from intermediate C. Thermal reaction of **2** with benzene does not lead to **1**, which can be explained either in terms of a high barrier for benzene coordination to form C or, more reasonably, by the lack of isocyanide lability in C following the rapid and reversible coordination of benzene. It is possible that photochemical formation of **1** from **2** in benzene<sup>21</sup> involves labilization of isocyanide from intermediate C rather than from **2**. Since C is not observed, its formation must be thermodynamically uphill from **2**.

### Conclusions

The reductive elimination of benzene from Tp'Rh(H)(Ph)-(CN-neopentyl) (**1**) in the presence of added neopentyl isocyanide has been shown to proceed by an associative mechanism. A kinetic isotope-labeling study has provided evidence that the reductive elimination of benzene is reversible. A mechanism is proposed which involves initial reductive elimination of benzene from **1** to give an  $\eta^2$ -benzene intermediate in which the rhodium atom can rapidly migrate around the  $\pi$ -system of the coordinated benzene. Associative displacement of the benzene with isocyanide occurs in a second step.

### Experimental Section

**General Procedures.** All operations and routine manipulations were performed under a nitrogen atmosphere, either on a high-vacuum line using modified Schlenk techniques or in a Vacuum Atmospheres Corp. Dri-Lab. Tetrahydrofuran, benzene, and toluene were distilled from dark purple solutions of benzophenone ketyl. Benzene- $d_6$ , THF- $d_6$ , and toluene- $d_8$  were distilled under vacuum from dark purple solutions of benzophenone ketyl and stored in ampules with Teflon-sealed vacuum-line adapters.

All <sup>1</sup>H NMR spectra were recorded on a Bruker AMX400 NMR spectrometer. All chemical shifts are reported in ppm ( $\delta$ ) relative to tetramethylsilane and referenced to the chemical shifts of residual solvent resonances (C<sub>6</sub>H<sub>6</sub>,  $\delta$  7.15; THF,  $\delta$  3.58, 1.73; toluene,  $\delta$  2.09). All temperatures for variable-temperature NMR spectroscopy were calibrated relative to the chemical shift differences in the NMR spectra of known standards (298–386 K, 80% ethylene glycol in DMSO- $d_6$ ; 298–228 K, 4% methanol in methanol- $d_4$ ). All UV-vis measurements were conducted on a Hewlett-Packard 8452A diode array spectrophotometer in conjunction with a PC using Hewlett-Packard 89531A spectrophotometer software. All measurements were conducted using a thermoregulating cell holder attached to a circulating constant-temperature water bath. All kinetics plots and least squares error analysis of rate data were done using Microsoft Excel. Analyses were obtained from Desert Analytics.

The preparation and characterization of **1**,<sup>21</sup> **2**,<sup>20</sup> **4**,<sup>21</sup> and **5**<sup>21</sup> have been previously reported. 2,6-Xylyl isocyanide was purchased from Strem Chemicals, Inc., and used as received. Neopentyl isocyanide was prepared by a literature procedure<sup>22</sup> and stored in a drybox at -20 °C to prevent polymerization. Sodium bis(methoxyethoxy)aluminum hydride (Red-Al) was purchased as a 3.4 M solution in toluene from Aldrich Chemical Co. and diluted to 0.34 M with THF prior to use. Silica gel plates used in the preparative thin-layer chromatography were purchased from Analtech and contained a fluorescent indicator.

**Preparation of Tp'Rh(H)(Ph)(CN-2,6-xylyl) (**3**).** A solution of 10 mg (0.013 mmol) of Tp'Rh(CN-2,6-xylyl) ( $\eta^2$ -PhN=C=N-2,6-xylyl) in benzene was irradiated for 1 h with high-intensity light ( $\lambda > 345$  nm). The solvent was removed in vacuo to give the product along with 1 equiv of PhN=C=N-2,6-xylyl. <sup>1</sup>H NMR (C<sub>6</sub>D<sub>6</sub>, 60 °C):  $\delta$  -13.251 (d,  $J$  = 24 Hz, 1 H, Rh-H), 1.869 (s, 3 H, pz CH<sub>3</sub>), 2.019 (s, 3 H, pz CH<sub>3</sub>), 2.116 (s, 3 H, pz CH<sub>3</sub>), 2.221 (s, 3 H, pz CH<sub>3</sub>), 2.228 (s, 6 H, aryl CH<sub>3</sub>), 2.325 (s, 3 H, pz CH<sub>3</sub>), 2.337 (s, 3 H, pz CH<sub>3</sub>), 5.544 (s, 1 H, pz H), 5.629 (s, 1 H, pz H), 5.774 (s, 1 H, pz H), 6.5–7.5 (8 H, aryl H).

**Thermolysis of **1** in Benzene- $d_6$ .** A stock solution of **1** was prepared by dissolving 20 mg (0.035 mmol) in 2.0 mL of benzene- $d_6$ . The solution was divided among four 5-mm NMR tubes. The samples were heated at 353, 367, 373, and 386 K, respectively, and <sup>1</sup>H NMR spectra were periodically obtained. Because the rate of reaction **2** was slow at 353 K, this particular sample was heated in an oven whereas the rate at the other temperatures was sufficiently fast that the samples could be heated directly in the NMR probe. The decrease in the integration of the hydride resonance at  $\delta$  -13.650 relative to the integration of the pyrazole hy-

drogen resonance at  $\delta$  5.540 was used to determine the rate of incorporation of benzene- $d_6$  into **1**. The ln (hydride integration) vs time plots at each temperature provided the rates given in Table I, which were used in the Eyring plot of Figure 1. Least squares analysis of the best line through the points gave a slope of -19023  $\pm$  543 and a y-intercept of 35.2  $\pm$  1.4, from which  $\Delta H^\ddagger$  = 38  $\pm$  1 kcal/mol and  $\Delta S^\ddagger$  = 23  $\pm$  3 eu were determined.

**Thermolysis of **1** in the Presence of Neopentyl Isocyanide. NMR Experiment.** A 10-mg (0.017-mmol) sample of **1** was dissolved in 0.5 mL of a 0.167 M solution of neopentyl isocyanide in benzene- $d_6$ . The solution was added to a 5-mm NMR tube attached to a vacuum line adapter with a Teflon-sealed stopcock. The solution was freeze-pump-thawed, and then the tube was flame sealed under 1 atm of nitrogen. The tube was heated in the NMR probe at 367 K, and <sup>1</sup>H NMR spectra were obtained every 12 min. The decrease in the integration of the hydride resonance was measured relative to an internal standard of silicone grease.

**UV-Vis Experiments.** A sample of **1** (6.0 mg, 0.104 mmol) was carefully weighed into a 10.0-mL volumetric flask, and benzene was added up to the line, giving a 1.0 mM solution of **1**. A 0.45-mL aliquot of this standard solution was placed in a 1 mm path length quartz cell which had a Teflon-sealed stopcock. To this solution was added directly either 2.8, 5.6, 10.0, 19.0, or 28.0  $\mu$ L of neopentyl isocyanide to give solutions of concentrations 52, 104, 186, 353, and 520 mM in isocyanide, respectively. The solutions were heated in the temperature-controlled cell holder in the UV-vis spectrophotometer at 82 ( $\pm$ 1) °C, and the increase in absorbance at 372 nm due to formation of **2** was monitored as a function of time over an estimated 3 half-lives for the reaction. An equilibrium absorbance value at 372 nm was determined from first-order modeling of the absorbance vs time data with Hewlett-Packard kinetics software (89531A operations software for the 8452A spectrophotometer). The equilibrium value at 372 nm was then used along with the absorbance vs time data to generate logarithmic plots from which  $k_{\text{obs}}$  could be determined from the slope (Table II). A plot of  $1/k_{\text{obs}}$  vs  $1/[\text{neopentyl isocyanide}]$  was linear. Least squares analysis of the best line through the points gave a y-intercept of 1588  $\pm$  433 s, which resulted in a  $k_1$  of 6.3 (1.7)  $\times 10^{-4}$  s<sup>-1</sup>.

**Determination of Thermodynamic Parameters for Thermolysis of **1** in Benzene in the Presence of Neopentyl Isocyanide.** Four identical samples were prepared by placing 0.45-mL aliquots of the stock 1.0 mM solution prepared above in a 1-mm path length quartz UV-vis cell along with 5.6  $\mu$ L of neopentyl isocyanide (104 mM in isocyanide). The samples were heated in the temperature-controlled cell holder of the UV-vis spectrophotometer at 338, 343, 350, and 356 K, and the absorbance at 372 nm was measured as a function of time over an estimated 3 half-lives of reaction. The equilibrium absorbance and  $k_{\text{obs}}$  determinations at each temperature were conducted as described above. A plot of ln ( $k_{\text{obs}}/T$ ) vs  $1/T$  gave a slope of -7645  $\pm$  610 and a y-intercept of 5.8  $\pm$  1.5, from which  $\Delta H^\ddagger$  = 15.2  $\pm$  1.2 kcal/mol and  $\Delta S^\ddagger$  = -36  $\pm$  3 eu were determined for reaction **3**.

**Kinetic Isotope Effect for Thermolysis of **1** in the Presence of Neopentyl Isocyanide in Benzene.** The complex Tp'Rh(D)( $d_5$ -Ph)(CN-neopentyl) was prepared by direct photolysis of Tp'Rh(CN-neopentyl)<sub>2</sub> in benzene- $d_6$ . A standard 1.7 mM solution of **1-d<sub>6</sub>** was prepared. A sample was prepared by placing 0.45 mL of the stock solution into a 1-mm quartz UV-vis cell with a Teflon stopcock along with 5.6  $\mu$ L of neopentyl isocyanide. The sample was heated at 82 °C, and the absorbance at 372 nm was measured every 10 min for a total of 15 h. Analysis of the absorbance vs time data was identical to that described above. The  $k_{\text{D}}$  used in the calculation of the kinetic isotope effect was an average of three separate runs as shown in Table IV. As a check for reproducibility, a second determination of  $k_{\text{obs}}$  for the reaction of **1** at 82 °C in 104 mM neopentyl isocyanide in benzene was made after completion of the  $k_{\text{D}}$  reactions. The average of this rate along with the  $k_{\text{obs}}$  obtained in this isocyanide concentration dependence experiment (Table II) was used in the determination of  $k_{\text{H}}$  (Table IV).

**Isocyanide Exchange in **1**.** A solution of 10 mg (0.017 mmol) of **1** in 0.5 mL of benzene- $d_6$  along with 22 mg (0.17 mmol) of 2,6-xylyl isocyanide was added to a 5-mm NMR tube containing a ground-glass joint connected to a vacuum-line adapter. The sample was freeze-pump-thawed on the vacuum line, and then the tube was flame-sealed under 1 atm of nitrogen. The sample was heated in the NMR probe at 60 °C, and <sup>1</sup>H NMR spectra were acquired every 30 min for a total of 4.5 h. Examination of the spectra showed no evidence of a resonance at  $\delta$  -13.251 or any other resonances corresponding to Tp'Rh(H)(Ph)(CN-2,6-xylyl) (**3**) over the course of the conversion of **1** to Tp'Rh(CNR)<sub>2</sub> (R = equilibrium mixture of neopentyl and 2,6-xylyl).

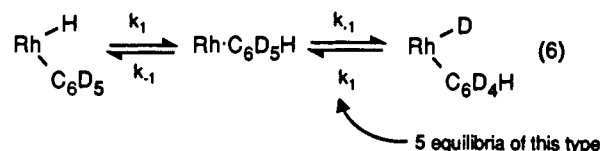
**Preparation of Tp'Rh(H)( $d_5$ -Ph)(CN-neopentyl) (**1-d<sub>5</sub>**).** A yellow solution of 60 mg (0.087 mmol) of Tp'Rh(CN-neopentyl)( $\eta^2$ -PhN=C=N-neopentyl) (**5**) in 2 mL of benzene- $d_6$  was irradiated with  $\lambda > 345$  nm light for 20 min. To the resulting pale yellow solution was added 0.25

mL of bromoform, and the reaction was stirred for 1 h. The solvent was removed in vacuo, and the crude product was purified by preparative thin-layer chromatography (2000- $\mu$ m silica gel on a 20  $\times$  20 cm<sup>2</sup> glass plate, 5:1 hexane:THF eluent). Yield of Tp<sup>+</sup>Rh(Br)(d<sub>5</sub>-Ph)(CN-neopentyl) (6): 40 mg (70%) of white solid.

To a solution of 40 mg (0.0607 mmol) of 6 in 3 mL of THF at 25 °C was added dropwise 0.5 mL of a 0.34 M solution of sodium bis(methoxyethoxy)aluminum hydride (Red-Al) in toluene. The resulting reaction mixture was stirred for 1 h, and then 7 mL of hexanes was added. The reaction was filtered twice through a 1 cm deep plug of silica gel in a 2.5 cm diameter fritted-glass funnel using vacuum. The silica was rinsed with 5 mL of a 5:1 hexanes:THF solvent mixture, and the combined filtrates were evaporated in vacuo to give 30 mg (85% from 6; 60% from 5) of the desired product 1-d<sub>5</sub> as a white solid. <sup>1</sup>H NMR (C<sub>6</sub>D<sub>6</sub>):  $\delta$  -13.650 (d,  $J$  = 24 Hz, 1 H, Rh-H), 0.604 (s, 9 H, C(CH<sub>3</sub>)<sub>3</sub>), 1.896 (s, 3 H, pz CH<sub>3</sub>), 2.196 (s, 3 H, pz CH<sub>3</sub>), 2.130 (s, 3 H, pz CH<sub>3</sub>), 2.246 (s, 3 H, pz CH<sub>3</sub>), 2.342 (s, 3 H, pz CH<sub>3</sub>), 2.441 (s, 3 H, pz CH<sub>3</sub>), 2.741 (s, 2 H, NCH<sub>2</sub>), 5.540 (s, 1 H, pz H), 5.708 (s, 1 H, pz H), 5.844 (s, 1 H, pz H). No resonances were observed in the region between  $\delta$  6.9 and  $\delta$  8.1.

**Thermolysis of 1-d<sub>5</sub> in Tetrahydrofuran.** A solution of 20 mg of Tp<sup>+</sup>Rh(H)(d<sub>5</sub>-Ph)(CN-neopentyl) (1-d<sub>5</sub>) in 0.5 mL of THF-d<sub>8</sub> was added to a 5-mm NMR tube containing a ground-glass joint and a Teflon-sealed vacuum-line adapter. The solution was freeze-pump-thawed on a vacuum line and the tube flame-sealed under 1 atm of nitrogen. The sample was heated at 60 °C in an oven and removed every 30 min in order to obtain a <sup>1</sup>H NMR spectrum at -40 °C in a cooled NMR probe. The decrease in the integration of the hydride resonance at  $\delta$  -14.260 along with the increase in the phenyl resonances at  $\delta$  6.484 (ortho),  $\delta$  6.558 (meta),  $\delta$  6.684 (para),  $\delta$  6.801 (meta'), and  $\delta$  7.619 (ortho') vs an internal standard of silicon grease ( $\delta$  0.38) was monitored for a total time of 330 min. Additional spectra were acquired at 768, 1143, and 1683 min, after which time it was concluded that the reaction had reached

equilibrium. Data from this experiment was used to generate the plot in Figure 6. The area of the hydride resonance was plotted as  $\ln((A_t - A_{eq})/(A_0 - A_{eq})) = -k_{obs}t$ , and the areas of the phenyl singlets were plotted as  $\ln(1 - A_t/A_{eq}) = -k_{obs}t$  in determining the rate constants reported in Table V. The approach to equilibrium described in eq 6 can



be evaluated explicitly, using a steady-state assumption on the intermediate and neglecting isotope effects, showing that  $k_{obs} = k_1$ .

In a second part to this experiment, the tube was broken open and the solution was placed in a second sealed NMR tube along with 50  $\mu$ L of benzene-d<sub>6</sub>. This solution was heated as before, and the integrations of the hydride resonance and phenyl resonances of the isotopomers of 1-d<sub>5</sub> were monitored every 30 min for 240 min. No significant change in the integrations of the resonances occurred over this time period, and no formation of free benzene-d<sub>5</sub> was observed. Further heating for 15 h did not result in any change.

**Thermolysis of 1-d<sub>5</sub> in Toluene-d<sub>8</sub>.** A sample of 1-d<sub>5</sub> was prepared in toluene-d<sub>8</sub> and heated at 60 °C as described above. The changes in the integrations of resonances at  $\delta$  -13.610, 6.911, 7.284, and 8.080 were monitored every 30 min for a total of 330 min. It was not possible to monitor the change in integration for two of the phenyl isomers of 1-d<sub>5</sub> because they were obscured by residual toluene resonances. The hydride integration data were used to determine  $k$  as described above.

**Acknowledgment** is made to the U.S. Department of Energy (Grant DE-FG02-86ER13569) for support of this work.

## Mechanisms for the Reactions between Methane and the Neutral Transition Metal Atoms from Yttrium to Palladium

Margareta R. A. Blomberg,\* Per E. M. Siegbahn, and Mats Svensson

Contribution from the Institute of Theoretical Physics, University of Stockholm, Vanadisvägen 9, S-11346 Stockholm, Sweden. Received October 24, 1991

**Abstract:** Calculations including electron correlations have been performed for the oxidative addition reactions between methane and the whole sequence of second row transition metal atoms from yttrium to palladium. The lowest barrier for the C-H insertion reaction is found for the rhodium atom. Palladium has the lowest methane elimination barrier. The barrier height is governed by two factors. In the reactant channel low repulsion favors a low barrier, and in the product channel strong bond formation is important. The atomic state with lowest repulsion toward methane is the  $d^{n+2}$  state and the strongest bonds are formed to the  $d^{n+1}$  s state. For rhodium both these states are energetically low lying. Only palladium has a bound  $\eta^2$  precursor state on the ground state potential surface. Another interesting result is that the potential surface for the reaction between methane and the rhodium atom is remarkably similar to the potential surface for the reaction between methane and C1RhL<sub>2</sub>, which has been studied experimentally.

### I. Introduction

Selective C-H activation of saturated alkanes by transition metal catalysts is an important step in the transformation of the abundant, but inert alkanes to more useful products. Therefore a large number of studies, both experimental and theoretical have been performed to elucidate the mechanisms of C-H activation by transition metal complexes. In the present study the reactivity of the second row transition metals with methane is investigated. It is the first study where such a systematic comparison between a whole row of metals has been performed for all the steps in a chemical reaction. The comparison between a wide range of different metals has been found to be essential for the understanding of the factors determining the energetics of the reaction.

Two fundamentally different mechanisms for transition metal activation of hydrocarbon C-H bonds in solution have been established by experiment: (1) oxidative addition to a coordinatively

unsaturated metal center and (2)  $\sigma$ -bond metathesis to a metal alkyl or hydride. The present study is concerned with the oxidative addition mechanism. Only a few transition metals are represented among those metal complexes which have been observed to insert into C-H bonds in saturated hydrocarbons via an oxidative addition mechanism. The first observations of alkane C-H insertion in solution were made in 1982 for iridium complexes, where the active intermediates were believed to be coordinatively unsaturated fragments of the general formula Cp<sup>\*</sup>IrL (L = CO, PR<sub>3</sub>).<sup>1,2</sup> Shortly afterwards the analogous rhodium fragment (Cp<sup>\*</sup>RhL)

(1) (a) Janowicz, A. H.; Bergman, R. G. *J. Am. Chem. Soc.* **1982**, *104*, 352. (b) Janowicz, A. H.; Bergman, R. G. *J. Am. Chem. Soc.* **1983**, *105*, 3929.

(2) (a) Hoyano, J. K.; Graham, W. A. G. *J. Am. Chem. Soc.* **1982**, *104*, 3723. (b) Hoyano, J. K.; McMaster, A. D.; Graham, W. A. G. *J. Am. Chem. Soc.* **1983**, *105*, 7190.